Dynamic Monte Carlo Simulation of Polymerization of Amphiphilic Macromers in a Selective Solvent and Associated Chemical Gelation

Wenqi Lu and Jiandong Ding*

Key Laboratory of Molecular Engineering of Polymers of Chinese Ministry of Education, Department of Macromolecular Science, Fudan University, Shanghai 200433, China

Received June 19, 2006; Revised Manuscript Received August 23, 2006

ABSTRACT: Gel formation via polymerization of amphiphilic macromers with a soluble central block and two insoluble but polymerizable end groups was investigated by dynamic Monte Carlo simulation. A simplified free radical polymerization of coarse-grained self-avoiding macromers was modeled on lattices. The simulation reproduced the unexpected experimental phenomenon reported in the literature that polymerization of PEO-acrylate or PEO-diacrylate macromers proceeded quite fast in water in contrast to in organic solvents. The simulation confirmed that the enhancement of local concentration of the polymerizable groups in the micellar cores was responsible for the rapid polymerization of self-assembled macromers in a selective solvent. A straightforward criterion to determine an infinite gel network in a finite modeling system with the periodic boundary was also put forward. The gelling kinetics associated with polymerization of such macromers with "double bonds" at both ends was investigated. Fast chemical gelation of concentrated macromer solutions in a selective solvent was interpreted from both the rapid polymerization and the more bridges linking micelles. Hence, this paper illustrates a strong coupling between polymerization kinetics and self-assembled structures of amphiphilic monomers.

I. Introduction

Polymerization kinetics constitutes an ever-lasting important topic in polymer science since more than half a century ago.[1,2] As the associated theories and simulations of free-radical polymerization are concerned, many researchers have investigated the underlying polymerization mechanisms of monomers in melts or in good solvents.[3−10] Nevertheless, the modeling of free-radical polymerization of amphiphilic macromonomers or macromers in a selective solvent is rather limited. In contrast to it, an interesting experimental observation has been done one and a half decades ago.[11] It is well-known that polymerization of macromers (usually in an organic solvent) is relatively slow due to a low concentration of polymerizable groups. Ito et al. found, however, that the free radical polymerization of poly(ethylene oxide) (PEO) acrylate macromers proceeded surprisingly fast in water.[11] They interpreted this interesting phenomenon as a result of self-assembly of the macromers in water into micelles because PEO chains are hydrophilic and the polymerizable ends of these macromers are hydrophobic. Afterward, such an experimental phenomenon has been found in many pertinent cases by Ito's group,[12] Hubble's group,[13] the author's group,[14,15] and so on. An associated theoretical research is thus required.

Monte Carlo (MC) simulation has been applied to study free-radical polymerization in a great success.[5,8,16,17] However, the conventional MC simulation approach to model polymerization kinetics in polymer chemistry is, due to lack of sufficient spatial information on monomers, not suitable for the study of the topic of this paper. On the other hand, dynamic MC simulation has been widely used to study chain configuration and dynamics in polymer physics.[18] After introducing reaction into lattices, dynamic MC simulation is able to study ideal "living polymers" in dynamic equilibrium,[19] free-radical polymerization,[20] living ion polymerization,[20] condensation polymerization,[21] and interchain exchange reaction.[22,23] Nevertheless, we have not found any report concerning simulation of polymerization of amphiphilic macromers yet.

Dynamic MC simulation of lattice chains has been employed to study self-assembly of block copolymers or amphiphiles in a selective solvent.[24−32] By combining these studies with the free-radical polymerization of lattice monomers, this paper will investigate the kinetics of free-radical polymerization of amphiphilic macromers in a selective solvent mimicking coarse-grained PEO-diacrylate macromers in water. Recently, there are many published experimental works concerning micelle-related polymerization (but not limited to polymerization of macromers).[33−37] So, our simulation method and results might also be meaningful for understanding various polymerizations of monomers (including macromers) under a self-assembled state in selective solvents.

Not less important is the modeling of the associated hydrogel formation. Various hydrogels have been extensively investigated and might be applied in many fields, especially as biomedical materials.[38−42] However, it is very hard to experimentally characterize the internal structures of hydrogels in details. A computer simulation affords a unique tool to "visualize" and further investigate chain networks. Hence, this paper also aims to extend MC simulation into studies of gels, especially chemically cross-linked gels resulting from polymerization. As an important extension of the work by Ito et al., who used mono-end-capped PEO macromers,[11] Sawhney et al.[13] prepared hydrogels by polymerization of PEO macromers with the two hydroxy ends capped by acryloyl groups (PEO-diacrylate). The present paper is focused on polymerization of two-double-bond macromers into gel network in a selective solvent, as schematically presented in Figure 1.

This paper is organized as follows. Section II describes the basic lattice model of self-avoiding macromer chains and associated interaction potentials related to a selective solvent and a common athermal solvent. The approach of dynamic MC simulation to model chain relaxation and free radical poly-

* Corresponding author: Fax 86-21-65640293; e-mail jdding1@fudan.edu.cn.

10.1021/ma061356j CCC: $33.50
Published on Web 09/21/2006

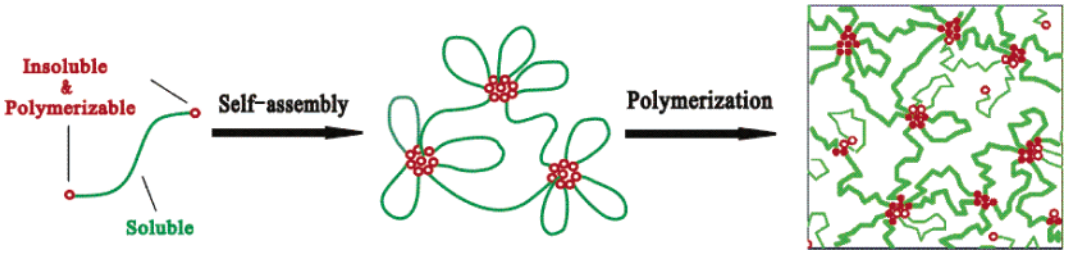

Figure 1. Two-dimensional schematic presentation of the system modeled in three dimensions: (left) an amphiphilic macromer with a soluble central chain end-capped by two insoluble polymerizable groups; (middle) core−corona micelles formed due to self-assembly of macromers in a selective solvent; (right) free-radical polymerization of macromers in the micellar state resulting in a chemical gel network emphasized by coarsened lines, whereas the thin lines represent those soluble central chains not belonging to any gel network. Blank and solid circles denote polymerizable and polymerized ends, respectively.

merization are also introduced. Section III presents simulation outputs of assembled structures, polymerization kinetics, and resulting chemical gelation. Significant differences of polymerization and gelling behaviors under the selective solvent and the athermal solvent are reproduced and further discussed. A summary is made in the last section.

II. Lattice Model and Dynamic MC Simulation Approach

II.1. Lattice Model of Amphiphilic Macromers. The coarse-grained bond fluctuation model[43,44] was employed to represent lattice chains. The idea of bond fluctuation originally proposed by Carmesin and Kremer[43] makes chains on simple cubic lattices behaving like quasi-off-lattice ones while keeping the high efficiency of a lattice simulation. This model has also been used in our group to study polymeric chains under shear flow,[45,46] coil−helix transition of a polypeptide,[47,48] and free-radical polymerization of ordinary (small molecular) monomers.[20] Each repeating unit of a macromer is presented by eight lattice sites in three dimensions. The periodic boundary condition is introduced along each dimension. An empty lattice site represents an implicit solvent particle. Chains are self-avoided. The bond intersection is also prohibited during each microrelaxation, if the permitted bond lengths are set as suggested by Deutsch and Binder.[44]

Since amphiphilic PEO-diacrylate macromers are modeled in this paper, we set two ends of a macromer as beads A while any remaining beads in a macromer as beads B. For a macromer with chain length N, the central block contains thus $N-2$ beads, and the coarse-grained macromer could be denoted as an $A_1B_{N-2}A_1$ triblock copolymer. As in most of lattice simulations, the interactions are considered only for those neighbor beads in contact including face-to-face, edge-to-edge, and corner-to-corner ways. Such a consideration of in-contact sites contains all of sites surrounding a cubelike bead. For an amphiphilic block copolymer, we introduce an attraction interaction between insoluble beads "under a selective solvent" with each pair of lattice sites among contacted beads A gained by a negative reduced energy ϵ_{AA} while all of other interaction pairs between A sites, B sites, and vacant sites are zero. Since the temperature effect will not be explicitly examined in this paper, we just use a reduced energy $\epsilon = \epsilon'/(k_BT)$, in which ϵ', k, and T denote the pair energy, the Boltzmann constant, and the Kelvin temperature, respectively. In the case of "under a common solvent", just the athermal state is modeled and thus all of interactions are set as zero.

II.2. Dynamic MC Simulation of Chain Relaxation and Micellization. No matter polymerization occurs or not, chain should be relaxed and self-diffuse. In dynamic MC simulation, a bead is selected randomly at first, and then a direction is chosen randomly for an attempt to move the bead. Supposing the athermal state, an attempt is accepted unless it violates either the excluded volume constraint or the allowed range of bond length. In the case of a nonathermal state, an attempt or a trial motion is accepted according further to the Metropolis importance sampling with the probability[49] $P = \min(1, e^{-\Delta E})$. Here, ΔE is the difference between the energies of the new (tried) and initial configurations in units of k_BT. A Monte Carlo step (MCS) is defined as the number of attempts for each bead to be chosen once on average. According to the kinetic interpretation of the Metropolis importance sampling based upon the master equation in statistics physics,[18] the sampling process reflects the kinetics of the underlying physics, namely, the number of MCS is linearly proportional to the physical time. So, such a MC simulation is called dynamic MC.

In this paper, the simulated system contains $64 \times 64 \times 64$ simple cubic lattices with the periodic boundary condition along each dimension. We set the length of macromer $N = 16$ and the number of chains $n_{ch} = 1024$, 512, 256, and 128 to make the volume fraction $\varphi = 0.50$, 0.25, 0.125, and 0.0625, respectively. At first, the macromers with a volume fraction φ were put in the lattice sites uniformly, and then a randomly distributed state was achieved at the athermal state after run for 10 million MCS. These random states were used as the initial states in the common athermal solvent in the forthcoming polymerization.

In a selective solvent, a series of temperatures or reduced energies were further tried from the athermal state to the lowest temperature, and a sufficiently long relaxation was performed to guarantee equilibrium at each temperature or reduced energy. During the relaxation procedure from the athermal state to the lowest temperature, the mean-square end-to-end distance and the contact number of AA were calculated, which demonstrates a transition from a homogeneous state to a micellar state. The following polymerization was examined upon the initial state at $\epsilon = 1.3\epsilon_c$, where ϵ_c is the reduced interaction potential among A beads just at the micellization transition point under each volume fraction.

In our simulation, a physical domain or an associate is thought to be formed once at least two insoluble beads are close to each other. The term "close" means formation of a face-to-face, edge-to-edge, or corner-to-corner contact. Self-assembled beads A constitute the "core" of that domain. A domain with number of core beads larger than seven is defined as a micelle in our simulation. When two insoluble ends of a macromer are in the same core, the central block of that macromer constitutes a "loop". A macromer looks like a "bridge" when their two ends belong to different cores.

II.3. Dynamic MC Simulation of Free Radical Polymerization. The dynamic MC could be extended to model both chain-diffusion process and polymerization kinetics. Just ir-

reversible reactions were modeled here. The initiation, propagation, and termination were considered, while chain transfer was neglected in this simulation. Termination was assumed to happen in the disproportionation way. The initiators were set as phantom. The molar ratio of phantom initiator to monomer [I]/[M] = 0.031. A constant initiation probability for each remaining initiator p_d was assumed throughout the polymerization process. Each initiation event produced two monomer radicals, which were selected randomly among the unreacted beads A in this simulation. A propagation event took place with a probability p_p when a radical bead met, along the randomly selected direction in an attempt, with a nearest-neighbor (face-to-face-contact) polymerizable bead or when a polymerizable bead met with a radical. Similarly, a termination event happened with a probability p_t when two nearest-neighbor radicals met with each other along the selected direction.

The probabilities of initiation, propagation, and termination were set as 10^{-6}, 10^{-3}, and 1, respectively. Both polymerization and chain relaxation were dealt with in each MCS. The total reaction time was taken to be from 1 million to 2 million MCS according to requirement. In each MCS, we first radicalized monomers with the preset initiation probability. Then a bead was selected randomly and tried to move according to the bond fluctuation model. If a radical hit a "double bond" (unreacted bead A), reaction occurred with the propagation probability; if two radicals met with each other, a disproportionation termination took place; then if a bead and a vacant site were selected, a chain relaxation was generated with the Metropolis acceptance probability; otherwise, nothing would happen, but this attempt was still included in record of a MC step. Because the functionality of a macromer is four (two beads A or two double bonds), a chemical gelation might occur due to cross-linking of macromers in the sampling process. Different from a physical domain, a "cluster" refers to a group of chemically linked macromers in this paper. The criterion of chemical gelation suitable for computer simulation will be suggested and discussed in the next section.

III. Results and Discussion

1. Transition from a Homogeneous State to a Self-Assembled Micellar State. Amphiphilic copolymers such as diblock and triblock copolymers exhibit self-assembly into micelles, etc., in a solvent which is selective to their constituents.[50−53] A PEO-diacrylate macromer is similar to a triblock copolymer. The insoluble ends as polymerizing groups in the macromers are, although very short compared to the central blocks, likely to be concentrated and organized in the micelle core, as suggested and experimentally confirmed by Ito et al.[11] This phenomenon was reproduced by our lattice dynamic MC simulation (Figure 2). The number of pairlike contact of end beads was employed to quantitatize the aggregation behaviors. With the increase of the absolute value of the reduced attraction energy or the decrease of temperature, a transition from a free-chain state to a micellar state was observed in our "computer experiment". This transition is reversible. The transition point is located at $\epsilon_{AA} = -0.46$ when the volume fraction $\varphi = 0.25$.

The transition point is dependent upon volume fraction of macromers. To make our following simulation results of polymerization under different concentrations comparable, the forthcoming polymerization was examined upon the initial state at $\epsilon \approx 1.3\epsilon_c$. In all of the cases, the free chains were found to be very few compared to the whole macromer chains, so most of the amphiphiles have been aggregated or associated into

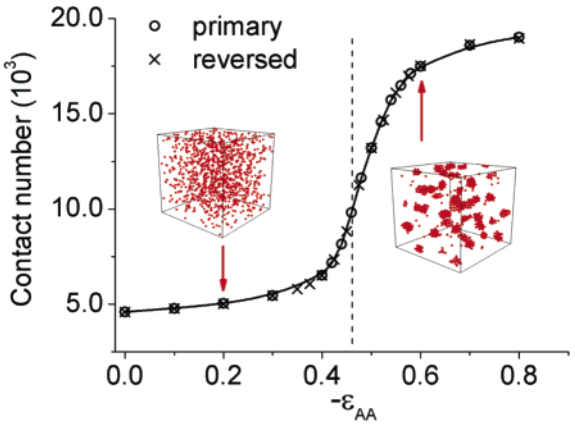

Figure 2. Averaged pair number of contact sites of insoluble ends in the equilibrium state vs the absolute value of the reduced potential for each A−A contact. The volume fraction $\varphi = 0.25$. Each trajectory was modeled from the athermal state to the lowest reduced energy in the primary process. 1 million MCS was used to reach equilibrium at each reduced energy, and then 100 thousand MCS was used for statistics. 20 independent trajectories were averaged. The dashed line indicates the transition point ϵ_c, which was determined from the peak of the differentiation of the curve. Insets are the snapshots under $\epsilon_{AA} = -0.20$ and -0.60 representing a free-chain state and a micellar state, respectively. Just beads A of the macromers are displayed. The reversed process was also examined, in which the reduced energy was increased from the lowest to zero.

Table 1. Number of Micelles n_{micel}, Number-Average Aggregation Number of Micelle n_{aggre}, and Weight-Average Aggregation Number of Micelle, w_{aggre}, under Different Volume Concentrations of Macromers ($\epsilon_{AA} = 1.3\epsilon_c$)

φ	$-\epsilon_{AA}$	n_{ch}	n_{micel}	n_{aggre}	w_{aggre}
0.50	0.48	1024	62.0	16.1	16.7
0.25	0.60	512	41.3	11.8	12.4
0.125	0.74	256	20.6	11.7	12.6
0.0625	0.82	128	8.7	14.5	14.9

micelles. The number of chains in each micelle, namely, the aggregation number of micelle, was then calculated on the basis of the output snapshots. Some basic data of the self-assembled state under four macromer concentrations are given in Table 1. The number of micelles n_{micel} was increased significantly with the amphiphile concentrations. It is also reasonable that the aggregation number, n_{aggre} or w_{aggre} is, different from micelle number, relatively not so sensitive to macromer concentration. The order of magnitude of the aggregation number or the number of chains in each micelle from our simulation is among a common range observed in experiments.[11]

2. Polymerization Kinetics of Macromers in a Selective Solvent and in the Common Athermal Solvent. Polymerization kinetics of the macromers in a selective solvent and a common solvent are shown in Figure 3 in a comparative way. In the case of a selective solvent, an attraction potential was introduced as $\epsilon_{AA} = -0.48$, -0.60, -0.74, and -0.82 corresponding to $\varphi = 0.50$, 0.25, 0.125, and 0.0625, respectively. In the case of the common solvent, just the athermal states were modeled for all of macromer concentrations. Under each macromer concentration, the free radical polymerization in the selective solvent proceeded faster than that in the athermal solvent (Figure 3).

It is well-known that macromer polymerization is, as usual, quite slow due to a low concentration of polymerizable groups. About 15 years ago, Ito et al. found an interesting phenomenon that PEO-acrylate macromers could be photopolymerized unexpectedly fast in water.[11] This phenomenon was reproduced from our computer experiment. In any real experiment, it is

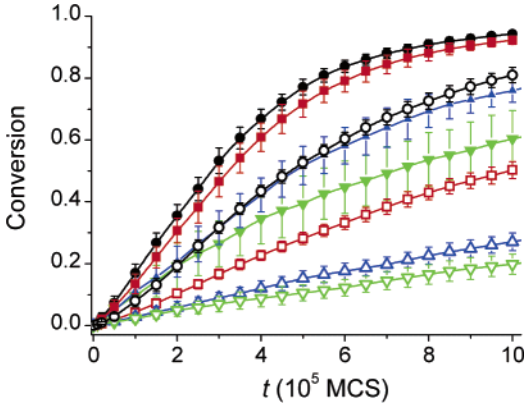

Figure 3. Conversion of macromers vs polymerization time under indicated macromer concentrations. [I]/[M] = 0.031. Filled symbols: selective solvent; open symbols: athermal solvent. Circle: $\varphi = 0.50$; square: $\varphi = 0.25$; triangle: $\varphi = 0.125$; inverted triangle: $\varphi = 0.0625$. In the case of selective solvent, $\epsilon_{AA} = 1.3\epsilon_c$ as indicated in Table 1. Error bars come from standard deviation calculated from 20 independent trajectories.

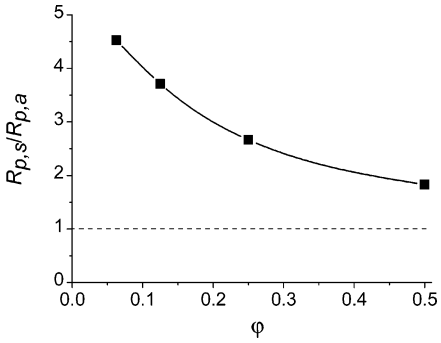

Figure 4. Ratio of polymerization rate in the selective solvent ($\epsilon_{AA} = 1.3\epsilon_c$) over that in the athermal solvent at each macromer concentration.

almost impossible to design controls with identical polymerization parameters (initiation, propagation, and termination constants) under water and any organic solvent. So, an idealized computer simulation has its own right to reveal the underling general mechanism theoretically. The acceleration of macromer polymerization in a selective solvent could be interpreted from the efficient enhancement of local concentrations of polymerizable groups after self-assembly of the amphiphilic macromers in a selective solvent if the polymerizable groups are eventually located in the cores of micelles.

The above viewpoint was further strengthened by Figure 4. While conversion in Figure 3 denotes the fraction of polymerized double bonds (end groups in this paper), the rate of polymerization R_p of macromers was determined from the initial slope of the curve of conversion vs time. The ratios of polymerization rates in the selective solvent ($R_{p,s}$) over those in the athermal solvent ($R_{p,a}$) under the associated macromer concentration are shown in Figure 4. All values are greater than 1 reasonably. We also found that the ratio was increased with the decrease of macromer concentration. This trend is consistent with that reported in the experiment by Ito et al.[11] Macromers under a homogeneous distribution in a good solvent should, at a low concentration, diffuse over a long average distance to collide with each other before a chain reaction is available. The decrease of termination rate is beneficial for acceleration of the global polymerization, but the decrease of propagation rate is less beneficial. A combinatory result leads to a globally slower polymerization under a lower monomer concentration, as is well-known in any textbook of polymer chemistry.[1,2] However, the effective concentration in the case of macromers is directly

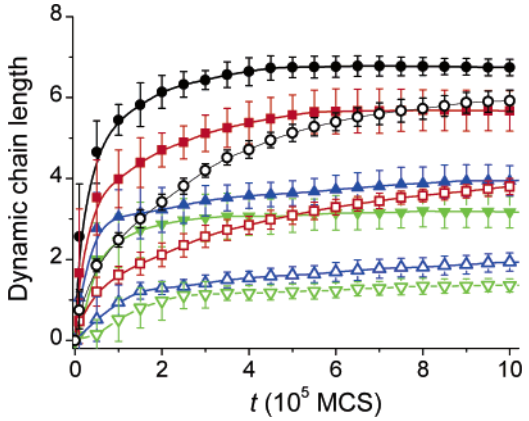

Figure 5. Dynamic chain length of "double bonds" at different solvents, concentrations, and polymerization time. Filled symbols: selective solvent; open symbols: athermal solvent. Circle: $\varphi = 0.50$; square: $\varphi = 0.25$; triangle: $\varphi = 0.125$; inverted triangle: $\varphi = 0.0625$. In the case of selective solvent, $\epsilon_{AA} = 1.3\epsilon_c$ as indicated in Table 1.

contributed by polymerizable groups instead of all repeating units in macromers. Different from the behavior in a common solvent (e.g., a suitable organic solvent for PEO-diacrylate macromers), the local concentration of polymerizable double bonds in the cores of micelles in a selective solvent (water for PEO-diacrylate) is, due to self-assembly, not so sensitive to the global concentration of macromers, which accounts for a higher contrast between two kinds of solvents under a lower macromer concentration (Figure 4). Therefore, self-assembly effects should be taken into consideration in amphiphilic monomers especially macromers, and polymerization of macromers might be influenced by aggregation states to a large extent.

Dynamic chain length is another important parameter in polymerization kinetics. Here, it just refers to the number of consecutive covalently linked beads A instead of degree of polymerization or molecular weight of a poly(macromer). Again, Figure 5 confirms that such an amphiphilic macromer exhibits different polymerization behaviors in a selective solvent from those in the athermal solvent. In the paper of Hubble and his colleagues,[13] they assumed that the consecutive polymerized ends in the network after polymerizing PEO-diacrylate macromers might be less than ten. So far, we have not found any straightforward experimental evidence in the literature. Now our simulation supports their estimation quite well. The simulation also reveals that even a few dynamic chain lengths are sufficient for formation of a chemical gel network.

3. Kinetics of Chemical Gelation. The time evolution of weight-average degree of polymerization of poly(macromer) (cluster size) is plotted in Figure 6. Here, a cluster is defined as a chemically linked poly(macromer). So, the molecular weight of the poly(macromer) (including both beads A and B) could be used to define "cluster size". Besides the information that the resulting molecular weight in the selective solvent is higher than that in the athermal solvent, the abrupt change of molecular weight at the later stage implies formation of a chemical gel. Figure 6 also shows the range of average molecular weight of micelles at the four volume concentrations. The value was obtained by chain length N times the aggregation number w_{aggre} in Table 1. According to Figure 6, the degree of polymerization of poly(macromer) might exceed the average molecular weight of micelles. So, for such macromers with two polymerizable ends, the micellar polymerization must include the intermicellar propagation. One big cluster consisting of connected micelles might lead to chemical gelation. Therefore, chemical gelling occurred in most of cases in Figure 6. Gel was, however, not

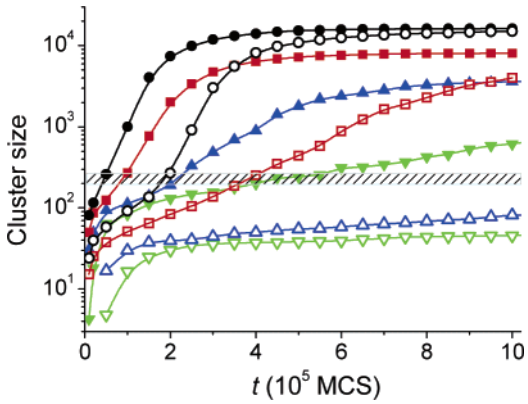

Figure 6. Weight-average cluster size of chemically linked macromers vs polymerization time. The shadow zone indicates the range of the weight-average molecular weight of micelles at the four examined macromer concentrations. Filled symbols: selective solvent; open symbols: athermal solvent. Circle: $\varphi = 0.50$; square: $\varphi = 0.25$; triangle: $\varphi = 0.125$; inverted triangle: $\varphi = 0.0625$. In the case of selective solvent, $\epsilon_{AA} = 1.3\epsilon_c$ as indicated in Table 1.

formed in the cases of $\varphi = 0.125$ and 0.0625 in the athermal solvent during our observation time, for we see from this figure that the resulting cluster sizes are far less than the average molecular weight of micelles. Thus, during formation of a cluster in these two cases, polymerization happened just within each isolated micelle.

A very large cluster might represent a gel network. Our viewpoint is that although it could be acceptable to use a cutoff cluster size to define a network, it is still much useful to suggest, if available, an absolute criterion to define an infinite network in simulation. However, the difficulty comes from the fact that any multiparticle simulation with a constant or finite density should be modeled in a finite-size system in any computer simulation. This paper put forward a direct approach to define an infinite chain network whenever the periodic boundary condition is employed. An infinite network must cross at least two opposite boundaries along at least one dimension; however, a cluster crossing boundaries might not belong to any infinite network but contain just an inner ring. Then, the key "calculation technique" is how to distinguish and thus exclude those boundary-crossing but finite clusters.

The suggested procedures suitable for programming are described as follows: (i) Select a self-closed cluster. One could try every bead in a cluster and search all of the possible routes to return to that bead. If no closed way could be found, the cluster is not self-closed. A typical case is shown in Figure 7a. (ii) Exclude all of inner-loop-like clusters. A typical case is displayed in Figure 7b. Supposing point P and point Q are two linked beads crossing the periodic boundary along one dimension, say, the x axis with the tried direction from P to Q, we define the basic crossing parameter as the sign function expressed as $s(\Delta x) = -1$ or $+1$ if $x(Q) - x(P) < 0$ or > 0 ($x \in [1, 64]$ in this paper.) The basic crossing parameters $s(\Delta y)$ and $s(\Delta z)$ along the other two dimensions are defined in a similar way. If in any closed search the summation along any dimension is nonzero, the cluster is an infinite network with a simple case shown in Figure 7c; otherwise, it is an inner closed ring (Figure 7b), in which $\sum s(\Delta x) = \sum s(\Delta y) = \sum s(\Delta z) = 0$ for all of possible self-closed search routes. Topological cross-link has not been dealt with in this paper.

It should be mentioned that Nguyen-Misra and Mattice[27] summarized and compared mainly three approaches to define a system composed of clusters as a network when they performed, under the periodic boundary condition, a simulation of physical gelation of ABA triblock copolymers. These approaches contain (1) divergence of weight-average cluster size, (2) increase of functionality in the largest cluster over two (the functionality is defined as the number of bridging chains over the number of micelles belonging to the cluster), and (3) a geometry definition, namely, passing through box boundaries in all dimensions, in which the third approach shares the similar physics to the criterion of the present paper. They found that the gel points determined by the first and second approaches ($\varphi_{gel,MW*}$ and $\varphi_{gel,\Phi*}$, respectively) basically agreed with each other albeit with a systematic difference ($\varphi_{gel,MW*} < \varphi_{gel,\Phi*}$). They also confirmed that the systems judged as a "gel" by the second approach did always satisfy the geometry condition while it was usually not the case at the volume fraction of $\varphi_{gel,MW*}$. Nevertheless, ref 27 did not directly employ the third approach to define a gel and then check the other two approaches. In fact, even a free chain located on the corner might possibly pass through box boundaries in one to three dimensions if the period boundary condition is used. A direct and practical geometry criterion is thus still open. The key of a direct geometry criterion is how to rule out the routine boundary crossing and any internal loop as indicated in Figure 7a,b. The present paper realizes the idea of the third approach in a straightforward way. We afford a mathematically rigorous and computationally available criterion for a cluster to be an infinite network in a finite system when the periodic boundary condition is employed. It is also worthy of noting that Nguyen-Misra and Mattice[27] addressed the possible significant influence of simulation box size on gel point unless the size was sufficiently large (over 30 in their simulation systems). Our simulation system with a box size of 64 has basically eliminated the box size effect on gel formation.

Our straightforward criterion of an infinite network allows for an unambiguous determination of onset time of gelling and calculation of gel content for each trajectory. The gel content is defined as the fraction of the number of beads in the chemically cross-linked infinite network over the total bead number. The ensemble averages of simulation outputs are shown in Figure 8. Different from the time-dependent behaviors of conversion (Figure 3), a transition related to chemical gelation was observed. The onset point (gel point) is also quite clear in Figure 8 (gel content determined on the basis of our straightforward gel criterion vs time) compared to that in Figure 6 (cluster size vs time). So, our criterion of an infinite network is, as an analytical tool in computer simulation, quite helpful for investigation of gel formation. Again, Figure 8 demonstrates that gelling of the amphiphilic macromers in a selective solvent is rather fast, which is reminiscent of the experiments of Hubble and his colleagues[13] and also of our own group.[14,15]

What is more, comparison between Figures 3 and 8 reveals that the difference between gelling rates in a selective solvent and in an athermal solvent is even more significant than that between polymerization rates. Gel contents at $\varphi = 0.125$ and 0.0625 are even kept zero in Figure 8 in the case of common solvent. The usual gelling behavior in a selective solvent is not merely an effect of acceleration of polymerization. Figure 9 illustrates unambiguously that even under the same conversion gel content in the selective solvent might be higher than that in the athermal solvent. Gelling occurred earlier in the selective solvent than in the athermal solvent, which implies that besides polymerization rate the gelling rates of the macromers in the selective solvent might be controlled by another factor. This factor is related to chain configuration according to our examination in the following subsection.

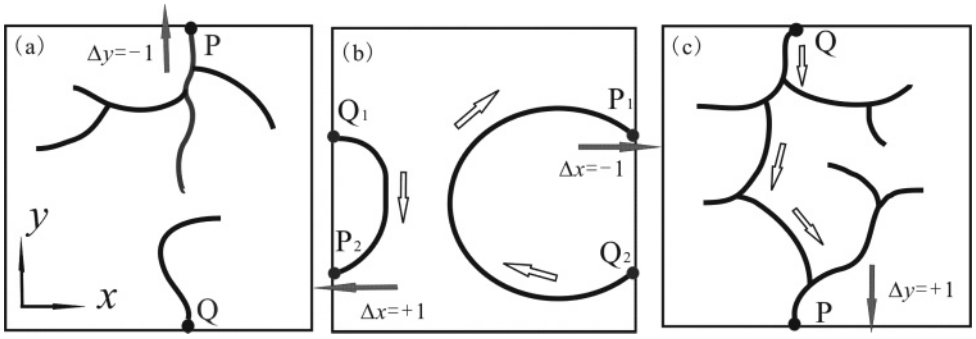

Figure 7. A two-dimensional schematic presentation of the criterion of a cluster as an infinite cross-linked network. (a) A nonclosed cluster, in which any bead cannot return to itself from any route, cannot be a gel network. Marked is the value of a sign function describing a boundary crossing from point P to point Q. (b) A self-closed cluster along the searching route starting from one of the solid-circle beads (P_1 or P_2) and researching along the marked arrows. A basic crossing parameter is set as the sign function as shown in the figure and described in the text. In the case of an inner ring, their summation in any closed search must be zero. (c) Another self-closed cluster determined as an infinite network considering the periodic boundary condition. At least one closed search is nonzero for an infinite network.

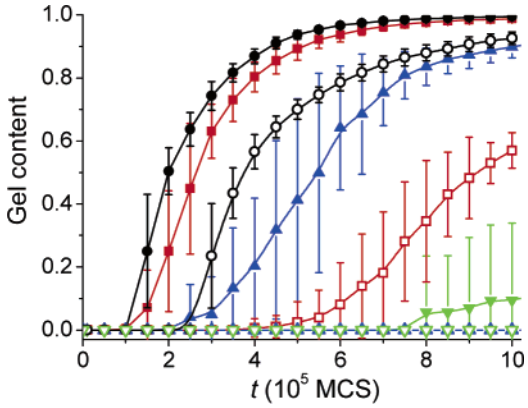

Figure 8. Gel content vs polymerization time under four macromer concentrations in a selective solvent (filled symbols) or in the athermal common solvent (open symbols). Circle: $\varphi = 0.50$; square: $\varphi = 0.25$; triangle: $\varphi = 0.125$; inverted triangle: $\varphi = 0.0625$. No gel was formed in the athermal solvent when $\varphi = 0.125$ and 0.0625. In the case of selective solvent, $\epsilon_{AA} = 1.3\epsilon_c$ as indicated in Table 1.

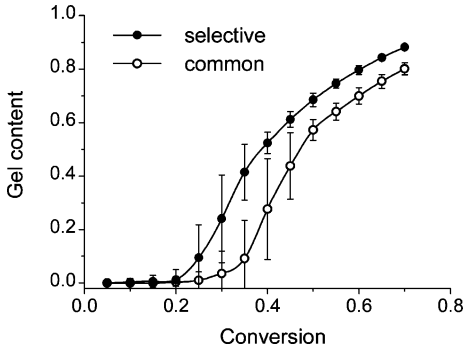

Figure 9. Gel content vs conversion in the selective solvent (filled symbols) or in the athermal common solvent (open symbols). $\varphi = 0.25$.

4. Spatial Structures of Macromers and Their Self-Assemblies. The polymerization of macromers in a selective solvent fixed the self-assembled structures of the amphiphiles, as shown in Figure 10. It is not hard to think that, besides the enhanced local concentration of polymerizable end groups, the chain configuration and supermolecular structures of the initial self-assembled state might affect the gelling kinetics.

Typical data of the distribution of the squared end-to-end distance before polymerization are shown in Figure 11. Macromers at the athermal state exhibited a unimodal distribution, which indicates that the chains are quasi-Gaussian random coils. In contrast to it, amphiphilic macromers in the selective solvent exhibited a bimodal distribution. So, the chain configuration

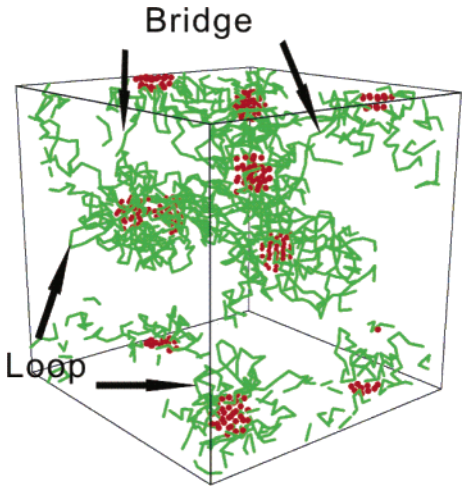

Figure 10. An exampled snapshot of a polymerizing system of amphiphilic macromers in a selective solvent. $\varphi = 0.0625$. The insoluble ends (beads A) are displayed as dots while the soluble central blocks composed of beads B are displayed as lines. Arrows mark typical central blocks acting as loops in one micelle or bridges linking two micelles.

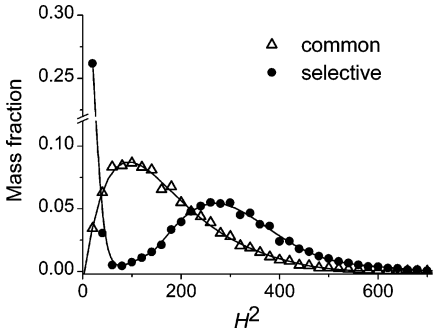

Figure 11. Mass fraction of macromers vs squared end-to-end distance of macromers in the selective solvent and in the athermal common solvent before polymerization. $\varphi = 0.25$.

has been significantly altered in the self-assembled state. The two peaks in the selective solvent correspond to loops and bridges, respectively. There are also some dangling chains (just one end in a micelle leaving another end free of any micelle). We found that the dangling chains were rare in the micellar state. As reported in the literature,[27−29] bridging among micelles plays an essential role in percolation (physical gelation) of associated triblock copolymers in selective solvents. Obviously, bridge is also extremely important for the formation of a chemically cross-linked gel network.

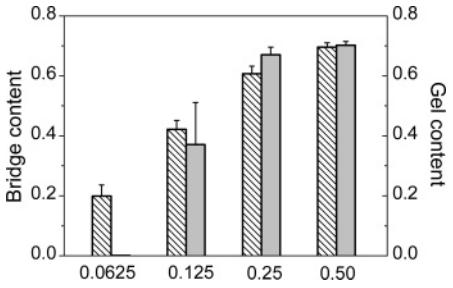

Figure 12. Bridge content (fraction of bridged macromers) in the selective solvent ($\epsilon_{AA} = 1.3\epsilon_c$) before polymerization (left normal coordinate) and gel content during polymerization at conversion ~0.50 (right) at marked macromer concentrations. At the most dilute concentration 0.0625, the gel content is zero when conversion is 0.50.

The fractions of bridged macromers in all of macromers at the four concentrations are shown in Figure 12. A more concentrated solution led to a higher fraction of bridged chains. The associated initial state with more bridges must be very beneficial for the formation of a gel network. Under the same conversion during polymerization or cross-linking reaction, a more concentrated solution resulted in a higher gel content. With increase of macromer concentration, gel content changes in a similar way to bridge fraction (Figure 12). So, the significant differences of gelling kinetics under different solvents and different concentrations in Figures 8 and 9 could be interpreted from both enhanced local concentration of polymerizable groups and the enhanced fraction of bridges of central blocks. These two effects are unified from the self-assembled spatial structures of the amphiphilic macromers.

IV. Summary

A dynamic MC simulation on simple cubic lattices was performed to study a simplified free radical polymerization of amphiphilic macromers in a selective solvent. Such a lattice simulation owns the great advantage of fruitful spatial information at the cost of computing time of a polymerization process, compared to the conventional MC simulation of free radical polymerization. Taking advantage of this simulation approach, the present paper reproduced the interesting phenomenon experimentally reported in the literature, namely, PEO-acrylate macromers were polymerized unexpectedly fast in water. Since each macromer in this paper contains two "double bonds", the polymerization could result in a chemically cross-linked gel. A straightforward criterion to determine an infinite polymeric network in a finite computer simulation system was also suggested, and gelling behaviors were then investigated.

Besides the contribution to the methodology of a computer simulation of polymerization kinetics related to microscopic and mesoscopic spatial structures, this paper shed more insight into micellar polymerization and associated chemical gelation. It has been confirmed that the enhancement of the local concentration of polymerizable and insoluble groups accounted for the acceleration of polymerization rate of the amphiphilic macromers in the selective solvent as compared to in the athermal solvent. As revealed by the simulation, the gelling kinetics is, compared to polymerization process, even more sensitive to medium types and macromer concentrations in the examined systems. Bridge content in the self-assembled state is very important for gel formation during micellar polymerization. Both microscopic chain configuration and mesoscopic supermolecular structures of the amphiphlic macromers have been changed with solvent and/or concentration. The polymerization kinetics and possible gelling of amphiphilic monomers are thus highly coupled to their self-assembled behaviors. Hence, the present paper strengthened that, as a classic topic of polymer chemistry, polymerization is sometimes closely related to the underlying polymer physics.

Acknowledgment. This work is supported by NSF of China (Nos. 50533010, 20574013, and a Two-Base Grant), the Key Grant of Chinese Ministry of Education (No. 305004), 973 Project (No. 2005CB522700), Science and Technology Developing Foundation of Shanghai (Nos. 04JC14019 and 055207082), and 863 Project from Chinese Ministry of Science and Technology.

References and Notes

(1) Flory, P. J. *Principles of Polymer Chemistry*; Cornell University Press: Ithaca, NY, 1953.
(2) Odian, G. *Principles of Polymerization*, 3rd ed.; Wiley-Interscience: New York, 1991.
(3) Beuermann, S.; Buback, M.; Hesse, P.; Lacik, I. *Macromolecules* **2006**, *39*, 184−193.
(4) Beuermann, S.; Buback, M.; Hesse, P.; Junkers, T.; Lacik, I. *Macromolecules* **2006**, *39*, 509−516.
(5) He, J. P.; Zhang, H. D.; Chen, J. M.; Yang, Y. L. *Macromolecules* **1997**, *30*, 8010−8018.
(6) Butte, A.; Storti, G.; Morbidelli, M. *Macromol. Theory Simul.* **2002**, *11*, 22−36.
(7) Tobita, H.; Mima, T.; Okada, A.; Mori, J.; Tanabe, T. *J. Polym. Sci., Part B: Polym. Phys.* **1999**, *37*, 1267−1275.
(8) Zetterlund, P. B.; Yamazoe, H.; Yamada, B. *Macromol. Theory Simul.* **2003**, *12*, 379−385.
(9) Jeszka, J. K.; Kadlubowski, S.; Ulanski, P. *Macromolecules* **2006**, *39*, 857−870.
(10) Iedema, P. D.; Hoefsloot, H. C. J. *Macromolecules* **2006**, *39*, 3081−3088.
(11) Ito, K.; Tanaka, K.; Tanaka, H.; Imai, G.; Kawaguchi, S.; Itsuno, S. *Macromolecules* **1991**, *24*, 2348−2354.
(12) Maniruzzaman, M.; Kawaguchi, S.; Ito, K. *Macromolecules* **2000**, *33*, 1583−1592.
(13) Sawhney, A. S.; Pathak, C. P.; Hubbell, J. A. *Macromolecules* **1993**, *26*, 581−587.
(14) Duan, S. F.; Zhu, W.; Yu, L.; Ding, J. D. *Chin. Sci. Bull.* **2005**, *50*, 1093−1096.
(15) Zhang, Y.; Zhu, W.; Wang, B. B.; Ding, J. D. *J. Controlled Release* **2005**, *105*, 260−268.
(16) Tobita, H. *Macromol. Theory Simul.* **2003**, *12*, 32−41.
(17) He, X. H.; Liang, H. J.; Pan, C. Y. *Macromol. Theory Simul.* **2001**, *10*, 196−203.
(18) Binder, K.; Heermann, D. W. *Monte Carlo Simulation in Statistical Physics*, 3rd ed.; Springer-Verlag: Berlin, 1997.
(19) Rouault, Y.; Milchev, A. *Phy. Rev. E* **1995**, *51*, 5905−5910.
(20) Lu, W. Q.; Ding, J. D. *Sci. China Ser. B: Chem.* **2005**, *48*, 459−465.
(21) Lu, W. Q.; Ding, J. D. *Acta Chim. Sinica* **2005**, *63*, 1231−1235.
(22) Jo, W. H.; Lee, J. W.; Lee, M. S.; Kim, C. Y. *J. Polym. Sci., Part B: Polym. Phys.* **1996**, *34*, 725−729.
(23) Jang, S. S.; Ha, W. S.; Jo, W. H.; Youk, J. H.; Kim, J. H.; Park, C. R. *J. Polym. Sci., Part B: Polym. Phys.* **1998**, *36*, 1637−1645.
(24) Wang, Y. M.; Mattice, W. L.; Napper, D. H. *Macromolecules* **1992**, *25*, 4073−4077.
(25) Xing, L.; Mattice, W. L. *Macromolecules* **1997**, *30*, 1711−1717.
(26) Kim, S. H.; Jo, W. H. *Macromolecules* **2001**, *34*, 7210−7218.
(27) Nguyen-Misra, M.; Mattice, W. L. *Macromolecules* **1995**, *28*, 1444−1457.
(28) Nguyen-Misra, M.; Mattice, W. L. *Macromolecules* **1995**, *28*, 6976−6985.
(29) Li, Y. Q.; Sun, Z. Y.; Shi, T. F.; An, L. J. *J. Chem. Phys.* **2004**, *121*, 1133−1140.
(30) Ji, S. C.; Ding, J. D. *Langmuir* **2006**, *22*, 553−559.
(31) Ding, J.; Carver, T. J.; Windle, A. H. *Comput. Theor. Polym. Sci.* **2001**, *11*, 483−490.
(32) Ji, S. C.; Ding, J. D. *J. Chem. Phys.* **2005**, *122*, 164901.
(33) Hill, A.; Candau, F.; Selb, J. *Macromolecules* **1993**, *26*, 4521−4532.
(34) Candau, F.; Regalado, E. J.; Selb, J. *Macromol. Symp.* **2000**, *150*, 241−249.
(35) Takasu, A.; Ohmori, S.; Yamauchi, Y.; Hirabayashi, T. *J. Polym. Sci., Polym. Chem.* **2002**, *40*, 4477−4484.
(36) Zhu, F. M.; Ngai, T.; Xie, Z. W.; Wu, C. *Macromolecules* **2003**, *36*, 7405−7408.
(37) Maiti, S.; Chatterji, P. R. *J. Colloid Interface Sci.* **2000**, *232*, 273−281.

(38) Hoffman, A. S. *Adv. Drug Delivery Rev.* **2002**, *54*, 3−12.
(39) Nowak, A. P.; Breedveld, V.; Pakstis, L.; Ozbas, B.; Pine, D. J.; Pochan, D.; Deming, T. J. *Nature (London)* **2002**, *417*, 424−428.
(40) Jeong, B.; Bae, Y. H.; Lee, D. S.; Kim, S. W. *Nature (London)* **1997**, *388*, 860−862.
(41) Yu, L.; Zhang, H.; Ding, J. D. *Angew. Chem., Int. Ed.* **2006**, *45*, 2232−2235.
(42) Flynn, L.; Dalton, P. D.; Shoichet, M. S. *Biomaterials* **2003**, *24*, 4265−4272.
(43) Carmesin, I.; Kremer, K. *Macromolecules* **1988**, *21*, 2819−2823.
(44) Deutsch, H. P.; Binder, K. *J. Chem. Phys.* **1991**, *94*, 2294−2304.
(45) Xu, G. Q.; Ding, J. D.; Yang, Y. L. *J. Chem. Phys.* **1997**, *107*, 4070−4084.
(46) Xu, G. Q.; Ding, J. D.; Yang, Y. L. *Polymer* **2000**, *41*, 3289−3295.
(47) Chen, Y. T.; Zhang, Q.; Ding, J. D. *J. Chem. Phys.* **2004**, *120*, 3467−3474.
(48) Chen, Y. T.; Zhang, Q.; Ding, J. D. *J. Chem. Phys.* **2006**, *124*, 184903.
(49) Metropolis, N.; Rosenbluth, A. W.; Rosenbluth, M. N.; Teller, A. H.; Teller, E. *J. Chem. Phys.* **1953**, *21*, 1087.
(50) Jain, S.; Bates, F. S. *Science* **2003**, *300*, 460−464.
(51) Liu, S. Y.; Hu, T. J.; Liang, H. J.; Jiang, M.; Wu, C. *Macromolecules* **2000**, *33*, 8640−8643.
(52) Korczagin, I.; Hempenius, M. A.; Fokkink, R. G.; Stuart, M. A. C.; Al-Hussein, M.; Bomans, P. H. H.; Frederik, P. M.; Vancso, G. J. *Macromolecules* **2006**, *39*, 2306−2315.
(53) Butun, V.; Top, R. B.; Ufuklar, S. *Macromolecules* **2006**, *39*, 1216−1225.

MA061356J